GEOPHYSICS, VOL. 84, NO. 2 (MARCH-APRIL 2019); P. A25–A29, 4 FIGS.
10.1190/GEO2018-0528.1

Comparison of geophone and surface-deployed distributed acoustic sensing seismic data

Kyle T. Spikes[1], Nicola Tisato[1], Thomas E. Hess[1], and John W. Holt[2]

ABSTRACT

The rapid and nonintrusive deployment of seismic sensors for near-surface geophysical surveys is of interest to make data acquisition efficient and to operate in a wide variety of environmental and surface-terrain conditions. We have developed and compared near-surface data acquired using a traditional vertical geophone array with data acquired using three different fiber optic cables operating in a distributed acoustic sensing (DAS) configuration. The DAS cables included a helically wrapped fiber, a nearly bare single-strand fiber, and an armored single-strand fiber. These three cables are draped on the ground alongside the geophones. Equivalent processing on colocated shot gathers resulted in a high level of similarity, in particular for reflection energy acquired through geophones and the helically wrapped cable. The single-strand fibers indicate much less similarity. Frequency content, however, differs in the raw and processed gathers from the geophones and the fiber optic cables. Nonetheless, results demonstrate that DAS technology can be used successfully to acquire near-surface reflection seismic data by deploying the cables on the surface. Potential applications for this technology include rapid deployment of active and/or passive arrays for near-surface geophysical characterization for various applications at different scales.

INTRODUCTION

This paper presents a unique near-surface seismic data set of vertical geophone data and data acquired with distributed acoustic sensing (DAS) fiber optic cables, with an emphasis on the reflections. The experiment included three separate DAS cables, one helically wrapped and two single strands. These cables were not buried in a shallow trench (e.g., Dou et al., 2017); rather, they were draped alongside the geophones on the surface. The data demonstrate the known directivity differences between a helically wrapped versus a single-strand cable. We demonstrate that near-surface reflection seismic data can be acquired using DAS technology by deploying the appropriate cable on the surface.

Rapid deployment of seismic sensors for subsurface characterization has been a goal for several decades. In addition to speed and efficiency, surface-terrain considerations might render one type of sensor or another more useful. Examples of this effort include the snow streamer (Eiken et al., 1989; Rygg et al., 1993), where a marine streamer with hydrophones acted as the seismic array on snow-covered glaciers. In much different settings, Bachrach and Mukerji (2001, 2004) use a portable dense 3D array of geophones. Use of land streamers (Spitzer et al., 2001; Van der Veen et al., 2001) and the autojuggie in 2D (Steeples et al., 1999; Spikes et al., 2005) showed how rapidly geophones could be deployed while recording seismic data. Subsequent versions of the autojuggie in 3D demonstrated that ultrashallow imaging could be done economically in various settings (Tsoflias et al., 2006; Miller et al., 2017).

These various approaches were limited in terms of the surface terrains in which they could be deployed. The snow streamer was used in only the one setting. Automated planting of geophones in 2D or 3D is easiest done where few to no surface obstacles are present. Furthermore, planting geophones is extremely difficult or impossible on hard surfaces such as compact soils, sands, gravels or surface rock layers, or pavement. An alternative to using geophones is accelerometers. However, they must be oriented properly and coupled to the ground sufficiently, and they require power. The newest seismic sensors are fiber optics used in DAS. DAS technology provides a measurement of strain over a given length of the fiber optic cable when the fiber is interrogated with a laser and timing instrument. DAS technology has been used in wellbores for vertical seismic profiling and calibration purposes (e.g., Mateeva et al.,

Manuscript received by the Editor 11 July 2018; revised manuscript received 28 October 2018; published ahead of production 13 December 2018; published online 13 February 2019.
[1]The University of Texas at Austin, Jackson School of Geosciences, Department of Geological Sciences, Austin, Texas, USA. E-mail: kyle.spikes@jsg.utexas.edu (corresponding author); nicola.tisato@jsg.utexas.edu; thomas_hess@mail.utexas.edu.
[2]The University of Arizona, Lunar and Planetary Laboratory and Department of Geosciences, Tucson, Arizona, USA. E-mail: jack.w.holt@gmail.com.

2014; Olofsson and Martine, 2017), imaging, (e.g., Harris et al., 2017), time-lapse monitoring (Correa et al., 2017; Mateeva et al. 2017), fracture detection (James et al., 2017), and inversion of elastic properties (Egorov et al., 2018). DAS has been used in surface deployments in various configurations and for various purposes (e.g., Daley et al., 2013; Bakulin et al., 2017; Castongia et al., 2017; Dou et al., 2017; Hornman, 2017; Jreij et al., 2017; Costley et al., 2018). Common among these surface deployments were the use of DAS cables buried in shallow (<1 m) trenches. Here, we demonstrate that DAS can be used for seismic investigations when the cable is draped on the surface.

EXPERIMENTAL SETUP

The field site was along a foot path in a city park west of Austin, Texas, on a Colorado River terrace composed of compacted, clay-rich soil a few meters deep overlying limestone bedrock. The compacted soil provided quite good geophone-to-ground coupling and direct contact with the DAS cables. The seismic experiment consisted of four parallel lines designed to acquire coincident 2D data in each line (Figure 1). The first line contained 96, 14 Hz geophones spaced at 1.5 m for a total line length of 142.5 m. Second was an approximately 160 m long helically wrapped DAS cable (provided by Silixa LLC) draped on the ground alongside the geophones. The pitch angle was 27° relative to the axial direction; the cable contained a jacketed central strength element with a nylon outer sheathing. This cable is deemed cable 1 for future reference. For the third line (cable 2), a nearly bare approximately 160 m long, straight, single-strand fiber was spliced to the helically wrapped cable. Last, the fourth line, about the same length as the other two (cable 3), was an armored, straight, single-strand fiber spliced to cable 2. Cable 3 was sheathed in a plastic coating. Each splicing location resulted in noise at the ends of each cable. The helically wrapped cable was originally part of a much longer cable intended for use in a wellbore study. The available length of it was the result of it being cut from the much longer cable. Accordingly, the major concern was that after unspooling this cable, it would coil up on itself. Out of extreme caution to this possibility, we deployed sand bags on the DAS cables every 9 m. This effort altered the coupling of the cables to the ground at the locations of the sand bags, but it did not necessarily improve the signal quality substantially.

Figure 1. The four coincident 2D seismic lines in the experiment. The geophone line consisted of 96, 14 Hz geophones at 1.5 m spacing. The blue cable is the helically wrapped cable, referred to as cable 1. The thin white one is a nearly bare single-strand fiber (cable 2). Cable 3 (black) is an armored single-strand fiber. The image shows approximately 80 cm of the three cables (the tape measure in yellow).

A Geometrics Geode system with four units recorded the data from the geophone line. An iDas2 interrogator system from Silixa LLC recorded the data from the three fiber optic cables. The seismic source was a 12 lb sledgehammer striking an aluminum plate. The sledgehammer was equipped with an accelerometer that served as the trigger generator. We acquired the trigger signal through a microcontroller-based board that generated two TTL signals suitable to activate the two systems simultaneously. The delay from the microcontroller-based board was measured in the laboratory using an oscilloscope and estimated at <10 μs. The time-sampling interval for the Geometrics Geode system was 1 ms with a 1 s recording time. The gauge length for the iDas2 system was 10 m with an interrogator sampling frequency of 10 kHz and a time sampling interval of 1 ms. The trace spacing was set to 1 m. Vertical stacking was four at each source location for the geophones and the three cables. We acquired data at 48 shot locations along the lines at a 3 m interval.

An important note is the major difference of duration of time for the deployments of the two systems. A crew of eight took approximately 45 min to plant the 96 geophones, string the take-out cables, clip in the geophones, and deploy the Geometrics Geodes and batteries and other associated cables. On the other hand, unspooling the helically wrapped cable and draping it alongside the geophones took approximately 5 min with the same number of people. The single-strand cables required a few minutes each to lay. Splicing of the DAS cables to each other took approximately 30 min.

DATA PROCESSING

We focus on the data from one coincident shot location from the four lines. Silixa applied proprietary denoising on the DAS data. After that, the processing steps included shot-signature deconvolution, normal moveout (NMO) correction, a Radon transform and filter to remove nonflattened events, and removal of the NMO correction. Specific to the shot-signature deconvolution, the method used was spectral estimation following Wilson-Burg (Fomel et al., 2003). The parabolic Radon transform served as a linear-velocity filter that removed the nonflattened events, in particular, the surface waves.

RESULTS

Data displayed are shot gathers and amplitude spectra for raw data, after shot-signature deconvolution, and after the Radon transform and filter. Figure 2a displays the geophone data, Figure 2b for cable 1, Figure 2c for cable 3, and Figure 2d for cable 4. Trace-to-trace gain was used for display. The offset ranges are not identical for the shot gathers due to slight differences in the lengths of the DAS cables and the geophone line, which also dictates the number of traces contained in each gather. In particular for cable 2, determining the exact location for the end of the cable versus the splice location proved difficult, which is why the negative offset range for that cable is shorter relative to cables 1 and 3. Rayleigh wave modes are present in each gather. Given the directivity of the DAS cables, i.e., Kuvshinov (2016), cable 1 (helically wrapped) contains vertical

and potentially horizontal components of the Rayleigh waves. Cables 2 and 3 (single strands) contain mostly the horizontal components. In the geophone data, the Rayleigh waves at short times and offsets are clipped, but not in the DAS data. The surface waves in the cable data also have a step-like appearance. Figure 2e contains the average amplitude spectra for the geophone and cable 1 data. The overall behavior is similar, but the cable 1 spectrum has some notches whereas the geophone spectrum is smooth. Spectra for cables 2 and 3 (Figure 2f) are quite similar.

Figure 3 shows the gathers and spectra after source-signature deconvolution. Each gather shows 0.25 s of data, different from Figure 2. In addition, the display gain is AGC with a 100 ms window. For the geophone data, the air wave is much more apparent in Figure 3a relative to Figure 2a. The clipped Rayleigh waves are also more apparent. In the cable data, high-frequency, nearly horizontal noise is present, particularly in cable 1 (Figure 3b–3d). The spectra in Figure 3e show some similarity up to approximately 110 Hz for the geophones and cable 1, although cable 1 demonstrates some notches. Greater than 110 Hz, the two spectra deviate. In Figure 3f, cable 2 clearly contains noise beginning at approximately 60 Hz. Cable 3 shows decaying frequencies at approximately 70 Hz.

Following the source-signature deconvolution, NMO correction was applied to flatten any hyperbolic events. The Radon transform was then applied, and any nonflattened events were filtered out, followed by removal of NMO correction. Figure 4 shows the four coincident shot gathers after these steps displayed with a 100 ms AGC operator. Figure 4a and 4b, geophone data and cable 1, respectively, contains significant reflection energy. The step-like behavior is present in some of the reflections in Figure 4b, and to some extent in Figure 4c and 4d. Although some possible reflection signal is present in Figure 4c and 4d, the coherency is much diminished relative to cable 1 and the geophone data. Reflection energy is possible in these cables at relatively short times and offsets if reflections have significant horizontal components. The apparently flat events at near offsets and long times are likely artifacts from the Radon transform. Figure 4e and 4f contains the average amplitude spectra for the gathers in Figure 4. In Figure 4e, the geophone and cable have notches but in different bands. Spectra for cables 2 and 3 still show similarity.

DISCUSSION

Data from the geophones and cable 1 clearly display differences in frequency content, apparent in the gathers and the spectra. Inherent response differences between geophones and the helically wrapped cable could in part explain the differences in the frequency content. Moreover, this cable is sensitive in its axial and radial directions, so it detects horizontal and vertical components of any arrival. Therefore, the recording is a composite of both components that might have different intrinsic frequency contents. A further complication in the interpretation of the data in cable 1 is the likely presence of S-waves, given its horizontal (axial) sensitivity. To separate and identify any composite recording, or S-waves, would require an independent horizontal measurement. In principle, the straight, single-strand fibers could provide this information if the data were of high enough quality. Last, the step-like behavior of surface waves in the raw data and in the reflections after the Radon transform could be due to the presence of the sand bags or to oversampling within the gauge length. The simpler explanation is that the sand bags cause these effects.

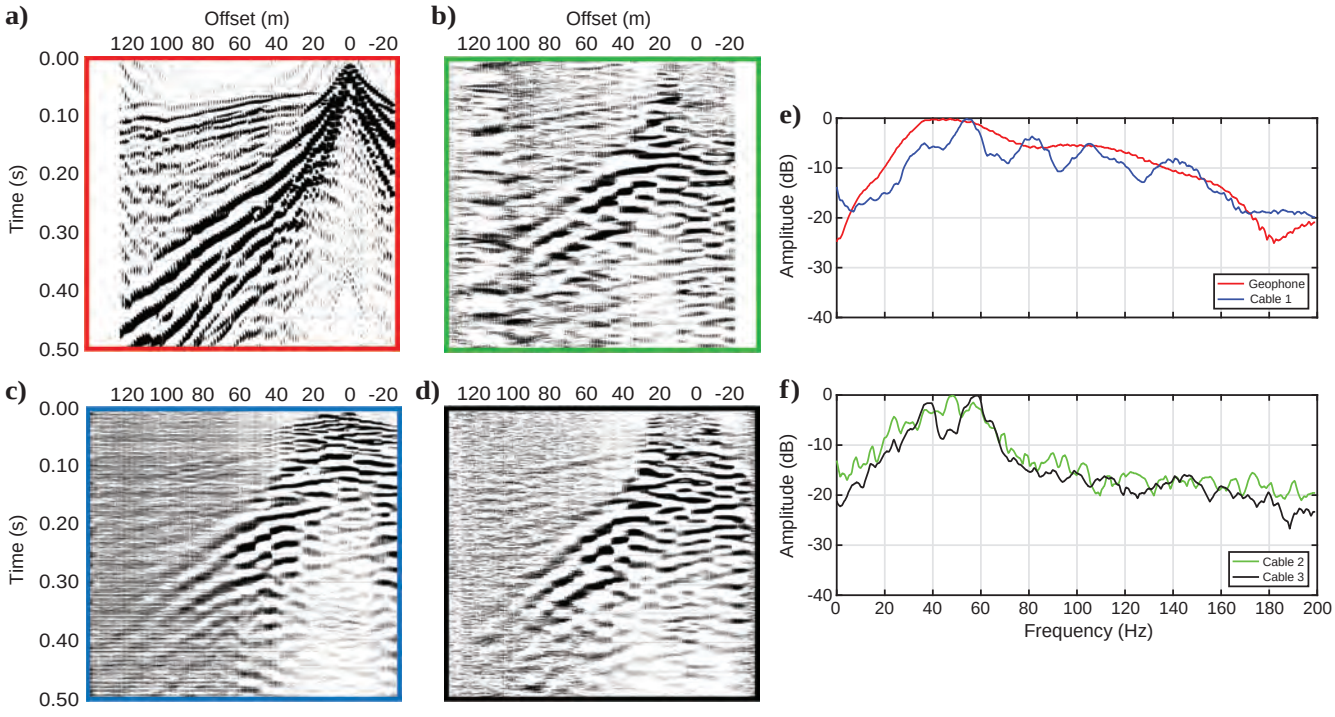

Figure 2. Raw shot gathers from the four lines. In (a) are the geophone data, (b) is for cable 1, (c) cable 2, and (d) cable 3. All four display Rayleigh wave energy for various modes. (e) and (f) are the average amplitude and spectra for the geophone and DAS data sets. Amplitude spectra show a similarity between the geophones and cable 1, and between cables 2 and 3. The color of the frames in (a-d) corresponds to the line colors in the spectral plots.

Future work with these data includes processing to obtain stacked sections for additional comparison. A separate study would be to perform surface wave spectral analysis on the comparative data. Numerical modeling will be required to understand the differences in boundary conditions of buried versus surface-deployed cables. Applications for this technique include rapid deployment of passive

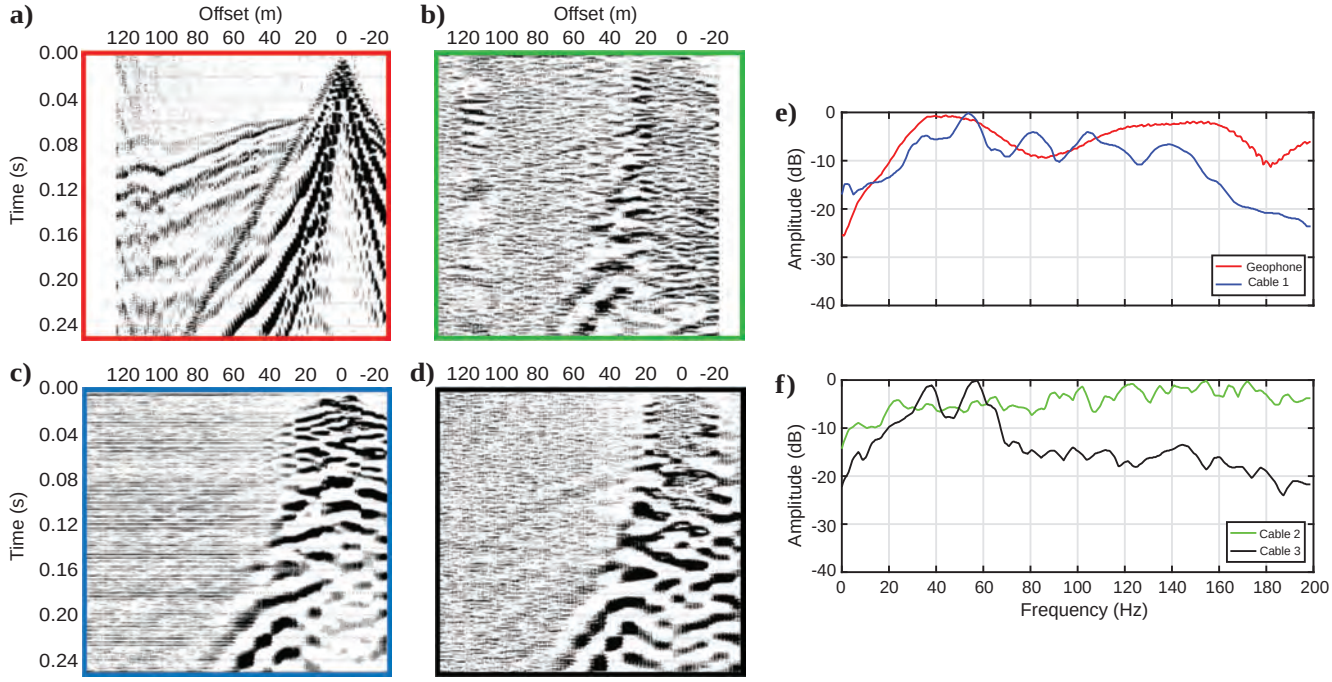

Figure 3. Gathers and amplitude spectra after applying shot-signature deconvolution. The juxtaposition is the same as in Figure 1. The gathers display 0.25 s of data.

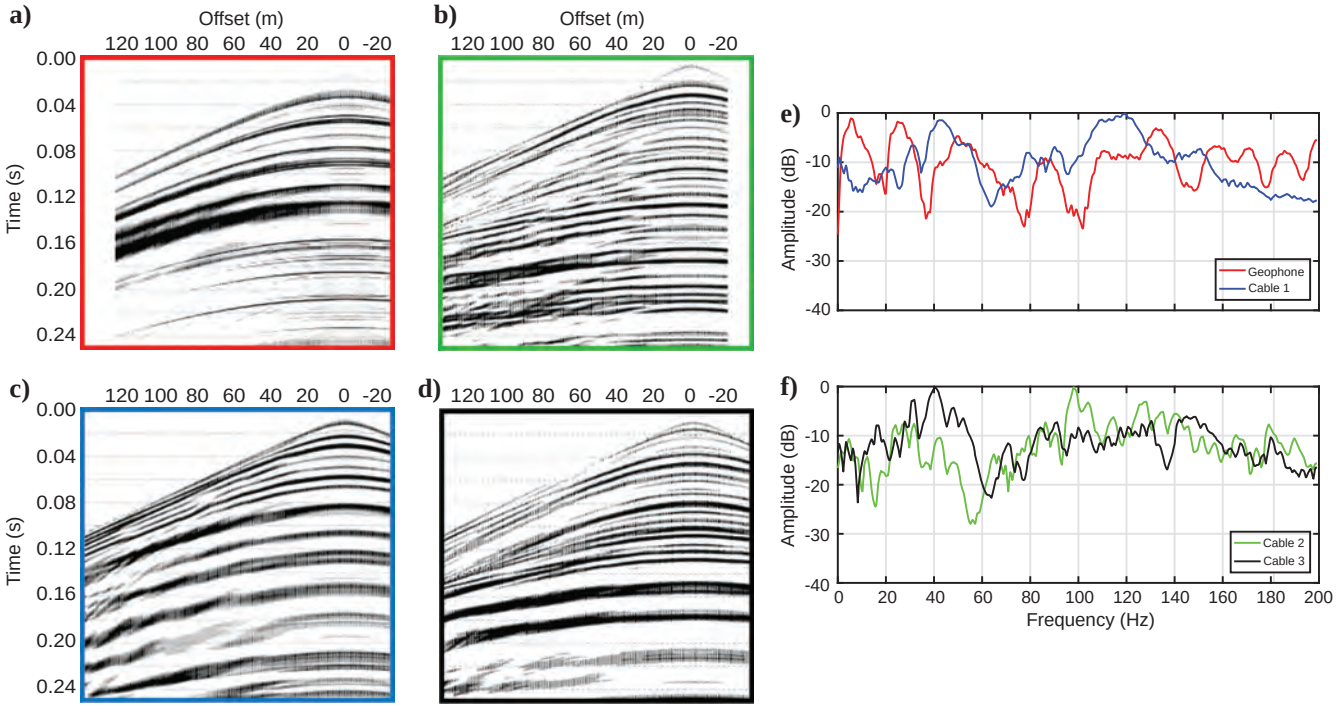

Figure 4. Shot gathers and amplitude spectra from the four lines after the Radon transform. This step reveals notable reflection energy in (a) the geophone data and (b) data from cable 1 (helically wrapped), which is expected given the directional sensitivity. Data in (c and d) show some hints of reflections but not nearly as coherent as in (b), as expected. The average amplitude spectra are in (e and f).

or active arrays for near-surface seismic characterization, civil and geotechnical-engineering investigations, environmental monitoring, and security and military operations. The system along with an active source could be mounted on an autonomous vehicle to acquire seismic data in locations dangerous for humans (e.g., on ice or radioactive locations). Such an autonomous vehicle potentially could be constructed for deployment to solid bodies in the solar system. Passive data could also be acquired. Alternatively, a rover-operated system could deploy DAS cable(s) on the surface and acquire active-source seismic data using a mounted impact source.

CONCLUSION

The purpose of this work was to compare conventional geophone data to data acquired with fiber optic cables in a DAS mode in a surface-based experiment. Results indicate that, from a qualitative standpoint, data from the helically wrapped DAS cable show a similarity to the geophone data. An important part of this similarity is the radial sensitivity of a helically wrapped cable. These data demonstrate that near-surface reflection seismic data can be acquired successfully using DAS technology by deploying the appropriate cable on the surface.

ACKNOWLEDGMENTS

We thank P. Ibisi, T. Martin, J. Greer, and T. Coleman for the assistance before and during data acquisition. Additionally, we thank the editors and three anonymous reviewers who provided excellent critiques that improved the manuscript. The authors wish to acknowledge and thank Paradigm University Grant Program of Emerson E&P Software for the use of Paradigm Echos for data processing in this project. We thank the City of Austin for allowing us to conduct this study in a city park. The Jackson School of Geosciences provided financial support for this work.

DATA AND MATERIALS AVAILABILITY

Data associated with this research are available and can be obtained by contacting the corresponding author.

REFERENCES

Bachrach, R., and T. Mukerji, 2001, Fast 3D ultra-shallow seismic reflection imaging using portable geophone mount: Geophysical Research Letters, **28**, 45–48, doi: 10.1029/2000GL012020.

Bachrach, R., and T. Mukerji, 2004, Portable dense geophone array for shallow and very shallow 3-D seismic reflection surveying. Part 1: Data acquisition, quality control, and processing: Geophysics, **69**, 1443–1455, doi: 10.1190/1.1836818.

Bakulin, A, P. Golikov, R. Smith, K. Erickson, I. Silvestrov, and M. Al-Ali, 2017, Smart DAS upholes for simultaneous land near-surface characterization and subsurface imaging: The Leading Edge, **36**, 1001–1008, doi: 10.1190/tle36121001.1.

Castongia, E., H. F. Wang, N. Lord, D. Fratta, M. Mondanos, and A. Chalari, 2017, An experimental investigation of distributed acoustic sensing (DAS) on lake ice: Journal of Environmental and Engineering Geophysics, **22**, 167–176, doi: 10.2113/JEEG22.2.167.

Correa, J., A. Egorov, K. Tertyshnikov, A. Bona, R. Pevzner, T. Dean, B. Freifeld, and S. Marshall, 2017, Analysis of signal to noise and directivity characteristics of DAS VSP at near and far offsets — A CO_2CRC Otway project data example: The Leading Edge, **36**, 994a1–994a7, doi; doi: 10.1190/tle36120994a1.1.

Costley, R. D., G. Galan-Comas, C. K. Kirkendall, J. E. Simms, K. K. Hathaway, M. W. Parker, S. A. Ketcham, E. W. Smith, W. R. Folks, T. W. Milburn, and H. M. Wadman, 2018, Spectral analysis of surface waves with simultaneous fiber optic distributed acoustic sensing and vertical geophones: Journal of Environmental and Engineering Geophysics, **23**, 183–195, doi: 10.2113/JEEG23.2.183.

Daley, T. M., B. M. Freifeld, J. Ajo-Franklin, S. Dou, R. Pevzner, V. Shulakova, S. Kashikar, D. E. Miller, J. Goetz, J. Henninges, and S. Lueth, 2013, Field testing of fiber-optic distributed acoustic sensing (DAS) for subsurface seismic monitoring: The Leading Edge, **32**, 699–706, doi: 10.1190/tle32060699.1.

Dou, S., N. Lindsay, A. M. Wagner, T. M. Daley, B. Freifeld, M. Robertson, J. Peterson, C. Ulrich, E. L. Martin, and J. B. Ajo-Franklin, 2017, Distributed acoustic sensing for monitoring of the near surface: A traffic-noise interferometry case study: Scientific Reports, **7**, 11620, doi: 10.1038/s41598-017-11986-4.

Egorov, A., J. Correa, A. Bóna, R. Pevzner, K. Tertyshnikov, S. Glubokovskikh, V. Puzyrev, and B. Gurevich, 2018, Elastic full-waveform inversion of vertical seismic profile data acquired with distributed acoustic sensors: Geophysics, **83**, no. 3, R273–R281, doi: 10.1190/geo2017-0718.1.

Eiken, O., M. Degutsch, P. Riste, and K. Rød, 1989, Snowstreamer: An efficient tool in seismic acquisition: First Break, **7**, 374–378, doi: 10.3997/1365-2397.1989021.

Fomel, S., P. Sava, J. Rickett, and J. F. Claerbout, 2003, The Wilson-Burg method of spectral factorization with application to helical filtering: Geophysical Prospecting, **51**, 409–420, doi: 10.1046/j.1365-2478.2003.00382.x.

Harris, K., D. White, and C. Samson, 2017, Imaging the Aquistore reservoir after 36 kilotonnes of CO_2 injection using distributed acoustic sensing: Geophysics, **82**, no. 6, M81–M96, doi: 10.1190/geo2017-0174.1.

Hornman, J. C., 2017, Field trial of seismic recording using distributed acoustic sensing with broadside sensitive fiber-optic cables: Geophysical Prospecting, **64**, 1–12, doi: 10.1111/1365-2478.12358.

James, S. R., H. A. Knox, L. Preston, J. M. Knox, M. C. Grubelich, D. K. King, J. B. Ajo-Franklin, T. C. Johnson, and J. P. Morris, 2017, Fracture detection and imaging through relative seismic velocity changes using distributed acoustic sensing and ambient seismic noise: The Leading Edge, **36**, 1009–1017, doi: 10.1190/tle36121009.1.

Jreij, S., W. Trainor-Guitton, and D. Miller, 2017, Field data comparison of 3D horizontal distributed acoustic sensing and geophones: 87th Annual International Meeting, SEG, Expanded Abstracts, 1–6, doi: 10.1190/segam2017-17793499.1.

Kuvshinov, B. N., 2016, Interaction of helically wound fiber-optic cables with plane seismic waves: Geophysical Prospecting, **64**, 671–688, doi: 10.1111/1365-2478.12303.

Mateeva, A., J. Lopez, D. Chalenski, M. Tatanova, P. Zwartjes, Z. Yang, S. Bakku, K. de Vos, and H. Potters, 2017, 4D DAS VSP as a tool for frequent seismic monitoring in deep water: The Leading Edge, **36**, 995–1000, doi: 10.1190/tle36120995.1.

Mateeva, A., J. Lopez, H. Potters, J. Mestayer, B. Cox, D. Kiyashchenko, P. Willis, S. Grand, K. Hornman, B. Kuvshinov, W. Berlang, Z. Yang, and R. Detomo, 2014, Distributed acoustic sensing for reservoir monitoring with vertical seismic profiling: Geophysical Prospecting, **62**, 679–692, doi: 10.1111/1365-2478.12116.

Miller, B. E., S. D. Sloan, G. P. Tsoflias, and D W. Steeples, 2017, The 3D Autojuggie: Automating acquisition of 3D near-surface seismic reflection data: Near Surface Geophysics, **15**, 3–11, doi: 10.3997/1873-0604.2016035.

Olofsson, B., and A. Martine, 2017, Validation of DAS data integrity against standard geophones — DAS field test at Aquistore site: The Leading Edge, **36**, 981–986, doi: 10.1190/tle36120981.1.

Rygg, E., P. Riste, A. Nøttvedt, K. Rød, and Y. Kristoffersen, 1993, The Snowstreamer — A new device for acquisition of seismic data on land: Norwegian Petroleum Society Special Publications, **2**, 703–709, doi: 10.1016/B978-0-444-88943-0.50047-2.

Spikes, K. T., P. D. Vincent, and D. W. Steeples, 2005, Near-surface common-midpoint seismic data recorded with automatically planted geophones: Geophysical Research Letters, **32**, L19302, doi: 10.1029/2005GL023735.

Spitzer, R., A. G. Green, and F. O. Nitsche, 2001, Minimizing field operations in shallow 3-D seismic reflection surveying: Geophysics, **66**, 1761–1773, doi: 10.1190/1.1487118.

Steeples, D. W., G. S. Baker, and C. Schmeissner, 1999, Toward the Autojuggie: Planting 72 geophones in 2 sec: Geophysical Research Letters, **26**, 1085–1088, doi: 10.1029/1999GL900191.

Tsoflias, G. P., D. W. Steeples, G. Czarnecki, and S. D. Sloan, 2006, 3-D Autojuggie: Automating deployment of two-dimensional geophone arrays for efficient ultra-shallow seismic-reflection surveys: Geophysical Research Letters, **33**, L09301, doi: 10.1029/2006GL025902.

Van der Veen, M., R. Spitzer, A. G. Green, and P. Wild, 2001, Design and application of a towed land-streamer system for cost-effective 2-D and pseudo-3-D shallow seismic data acquisition: Geophysics, **66**, 482–500, doi: 10.1190/1.1444939.